# Polarization of periodic degrees of freedom in response to cyclic transformations

Hadrien Vroylandt
*Laboratoire de Physique Théorique (UMR8627), CNRS, Univ. Paris-Sud, Université Paris-Saclay, 91405 Orsay, France*

Diego Frezzato*
*Department of Chemical Sciences, University of Padova, via Marzolo 1, I-35131, Padova, Italy*

(Received 14 February 2018; revised manuscript received 30 July 2018; published 4 October 2018)

When a classical fluctuating system in contact with a thermal bath undergoes a driven transformation in a finite time, a nonequilibrium distribution is created and an amount of energy is inevitably dissipated on average. It is known that the average dissipation and the extent of the out-of-equilibrium are mutually bounded. Here we elaborate the perspective of exploiting such a constraint to check the admissibility of the nonequilibrium distributions at a given amount of average dissipation. Namely, we focus on cyclic transformations and derive an upper bound for the statistical polarization that may be present, after the cycle, over an *a priori* unbiased periodic degree of freedom of the system. The finding is then applied to establish the maximum polarization that can be induced on the velocity of massive moieties in many-body molecular systems in response to generic cyclic transformations.

DOI: 10.1103/PhysRevE.98.042110

## I. INTRODUCTION

At the nanoscale, a system subjected to a guided transformation undergoes fluctuations due to the contact with the environment acting as thermal bath. At such a scale, the thermodynamics becomes "stochastic" since the erratic nature of the uncontrolled degrees of freedom makes that the amounts of work and heat exchanged by the system are stochastic variables with distributions characteristic of the transformation protocol [1]. After the early stage in which the pragmatic target was mainly charting the system's free energy in the space of the externally *controlled* parameters by exploiting the raw information contained in the work distribution function, ever-growing attention was given to relate the average amount of work, or more directly the average energy dissipation, with the dynamical response of the *uncontrolled* degrees of freedom. For example, emergent concepts like "self-adaptation" [2,3] and "nonequilibrium self-assembly" [4] refer to the system's structural organization induced by dissipative processes, and pertain to such aspects of stochastic thermodynamics.

The present work fits into such a context. In essence, the focus will be on investigating how a fixed amount of average dissipation constrains the admissible out-of-equilibrium distributions on the uncontrolled degrees of freedom at the end of a driven transformation starting from equilibrium conditions. In particular, we shall consider cyclic transformations performed on a system with a periodic internal degree of freedom, and explore the constraints on the statistical distribution for such a coordinate.

Let us introduce the problem. Consider a classical system fluctuating in contact with a thermal bath and undergoing a cyclic transformation driven by an external agent. Suppose that the system possesses a periodic continuous coordinate over which the statistical distribution at equilibrium is uniform. In the following, we shall use the expression "*a priori* unbiased degree of freedom" to address this situation. Such a rotational-like coordinate may correspond to a physical degree of freedom, or it may be an abstract coordinate in all generality. In response to a generic cyclic transformation, the marginal distribution over such a coordinate will develop a bias which, in this case, can be naturally termed as "statistical polarization." The question posed here is the following: Knowing *only* the average amount of energy put into play by the external agent, which is the maximum extent of statistical polarization that can be realized on such a kind of periodic degree of freedom?

To quantity the polarization we adopt a parameter $\mathcal{P}$ built with the averages of first-rank Fourier components. In the context of "directional statistics" [5], such a parameter is known as "mean resultant length" and is employed to quantify the concentration of orientational data with respect to the mean orientation. We shall see [statement (ii) in the following] that it is indeed possible to provide an upper bound for $\mathcal{P}$ only from the knowledge of the average amount of energy expended in the form of performed work; the details about external agent, system, and kind of transformation are irrelevant. In such a system-free framework, one can only state that $\mathcal{P}$ *cannot* exceed the upper bound, while no statements can be made about extent and orientation of the actual polarization realized case by case.

As a first application we shall consider the case of arbitrarily complex molecular systems made of massive pointlike moieties. By representing the velocity vector of a moiety in spherical coordinates, the azimuthal angle is exactly a periodic coordinate with uniform distribution at the thermal equilibrium. In response to a cyclic transformation, the velocity of each moiety will develop a polarized distribution onto an

*diego.frezzato@unipd.it

 

arbitrarily chosen "observation plane." Statement (iii) will concern the maximum extent of in-plane velocity polarization that can be realized given the amount of energy expended on average. In terms of an ensemble of system's replicas, all subjected in parallel to the same transformation, such a bound can be translated into the maximum extent of coherent movement that can be induced by a cyclic transformation.

## II. PRELIMINARIES

Let $\mathbf{x}$ be the set of relevant variables of the system (general configurational variables and, possibly, their conjugated momenta) whose fluctuations are supposed to be describable as a stochastic Markov process. For a state of thermal equilibrium, $p_{\rm eq}(\mathbf{x}) = Z^{-1} e^{-\beta V(\mathbf{x})}$ is the canonical distribution of the microstates, where $Z = \int d\mathbf{x}\, e^{-\beta V(\mathbf{x})}$ is the partition function with $V(\mathbf{x})$ the configurational energy and $\beta = (k_B T)^{-1}$ ($k_B$ is the Boltzmann constant and $T$ the absolute temperature of the thermal bath). The word "distribution" is used here with a twofold meaning: it may refer either to the probability density associated with the statistical expectation in a single-system view, or to the distribution of microstates in an ensemble context.

Now suppose that some external agent "picks" the system at equilibrium and performs a transformation by acting on some parameter(s) in a prescribed way. While the drive is active, the system remains in contact with the thermal bath. Let $p(\mathbf{x})$ be the distribution associated with the final state of the system. As customarily done, we adopt the relative entropy (Kullback-Leibler divergence [6]) to quantity the deviation of $p(\mathbf{x})$ from the "underlying" equilibrium distribution $p_{\rm eq}(\mathbf{x})$ at the final value of the controlled parameter(s):

$$\mathcal{D}(p||p_{\rm eq}) = \int d\mathbf{x}\, p(\mathbf{x}) \ln \frac{p(\mathbf{x})}{p_{\rm eq}(\mathbf{x})}. \tag{1}$$

The quantity $\mathcal{D}$ is non-negative and null only if $p(\mathbf{x})$ and $p_{\rm eq}(\mathbf{x})$ are coincident, that is, in the ideal case of absence of lag between system's response and external drive.

In driving the system with the prescribed schedule, the agent performs *work*. Due to the fluctuations of the uncontrolled degrees of freedom, the amount of work is a stochastic quantity. Let $\overline{w}$ be the average work, where the term "average" can be either intended as average over the ensemble of outcomes from the repetition of the same transformation or as probabilistic mean value in a single-system view. Since the transformation is conducted in a finite time, an amount of energy is, on average, inevitably dissipated (wasted) just for operating in out-of-equilibrium conditions. Such average dissipated energy, $\overline{w}_{\rm diss}$, corresponds to the difference between $\overline{w}$ and the variation of Helmholtz free energy (denoted by $A$) of the system in passing from the initial equilibrium state to the underlying equilibrium state associated with the final value(s) of the controlled parameter(s):

$$\overline{w}_{\rm diss} = \overline{w} - (A_1 - A_0), \tag{2}$$

where $A_i = {\rm const}(T) - \beta^{-1} \ln Z_i$ with $i = 0$ for the initial state and $i = 1$ for the final one; ${\rm const}(T)$ is an immaterial offset at the fixed temperature. The difference $A_1 - A_0$, which is required to get $\overline{w}_{\rm diss}$ from Eq. (2), can be obtained by the canonical partition functions [$A_1 - A_0 = -\beta \ln Z_1/Z_0$] or, as an empirical quantity, by Jarzynski's equality [1] if the full work distribution function $\rho(w)$ is available [$A_1 - A_0 = -\beta^{-1} \ln \int dw \rho(w) e^{-\beta w}$].

For cyclic transformations as those of interest here, the final underlying equilibrium state and the initial equilibrium state of the system do coincide, hence $A_1 = A_0$. This implies $\overline{w}_{\rm diss} \equiv \overline{w}$, i.e., the average energy dissipation is *directly* identified with the average work. Thus, in the following argumentation, the expressions "average work" and "average energy dissipation" (all referred to a cycle) can be freely interchanged [7].

## III. DISSIPATION AND NONEQUILIBRIUM DISTRIBUTION

The following remarkable inequality, which expresses a mutual bound between average dissipation and deviation from equilibrium, was derived by Vaikuntanathan and Jarzynski [8]:

$$\mathcal{D}(p||p_{\rm eq}) \leqslant \beta \overline{w}_{\rm diss}, \tag{3}$$

where the equality holds only in the quasistatic limit. This relation is valid regardless of the dynamical regime of the fluctuations, overdamped or underdamped in all generality. In a recent work [9], the same result, and even a stronger inequality regarding the *rates* of variation of the quantities in Eq. (3), was obtained from the Fokker-Planck equation describing the evolution of the nonequilibrium distribution during the transformation. For the validity of Eq. (3) it is only required that, even during the driven transformation, the dynamics of the uncontrolled degrees of freedom be a Markov process and that the micro-reversibility holds; these are the same assumptions invoked for the derivation of the main work fluctuation theorems in stochastic thermodynamics [1]. In passing, note that since $\mathcal{D}$ is non-negative, Eq. (3) implies the weaker inequality $\overline{w}_{\rm diss} \geqslant 0$, hence $\overline{w} \geqslant A_1 - A_0$; this is nothing but the Clausius inequality (one of the facets of the second principle of thermodynamics) formulated in terms of average quantities for fluctuating systems [1].

Equation (3) is rather general. In what follows we shall focus on cyclic transformations. In such a situation, Eq. (3) turns into

$$\text{Cyclic transformation}: \quad \mathcal{D}(p||p_{\rm eq}) \leqslant \beta \overline{w}. \tag{4}$$

Note that the time variable does not appear in the above relations. In fact, it is only meant that *some* finite-time transformation takes place, without the need to specify its actual schedule, i.e., the path in the space of the controlled parameter(s), the progression rate, and the duration.

Equation (4) [and, similarly, Eq. (3)] can be viewed from two angles. First, it tells us that if our target is the creation of a certain distribution $p(\mathbf{x})$ via a finite-time cycle, it is required for sure, regardless of the schedule, that an average amount of energy at least equal to $\beta^{-1}\mathcal{D}(p||p_{\rm eq})$ has to be put into play. On the other hand, if the involved average amount of energy (hence of average dissipation) is known, then only the distributions $p(\mathbf{x})$ that satisfy Eq. (4) are *admissible* and the following assertion can be done:

(i) *Once a cyclic transformation is performed on a system initially at thermal equilibrium, the distributions* $p(\mathbf{x})$ *that*

*violate* $\mathcal{D}(p||p_{\rm eq}) \leqslant \beta\overline{w}$ *are not compatible with the final statistical state of the system.*

In practice, if $p(\mathbf{x})$ is represented by a point in a multidimensional space of order parameters (statistical averages of functions of $\mathbf{x}$), then some regions of such a space are *surely* not allowed.

Remarkably, the inequalities Eqs. (3) and (4) are still valid if $\mathcal{D}(p||p_{\rm eq})$ is replaced by the relative entropy for the reduced distributions on fewer degrees of freedom. In fact, if $\mathbf{x} = (\mathbf{x}_1, \mathbf{x}_2)$ and $\rho(\mathbf{x}_1) = \int d\mathbf{x}_2\, p(\mathbf{x}_1, \mathbf{x}_2)$ is the reduced (marginal) distribution on the subset $\mathbf{x}_1$, then [10]

$$\mathcal{D}(\rho||\rho_{\rm eq}) \leqslant \mathcal{D}(p||p_{\rm eq}). \tag{5}$$

## IV. POLARIZATION OF SINGLE PERIODIC COORDINATES

### A. The general case

Let us assume that one of the degrees of freedom of the system is a periodic coordinate $\phi \in [0, 2\pi)$. Then, let $\rho_{\rm eq}(\phi)$ be the associated reduced equilibrium distribution, whereas $\rho(\phi)$ is the nonequilibrium distribution after *some* cyclic transformation. According to Eq. (4) with Eq. (5), it must be

$$\mathcal{D}(\rho||\rho_{\rm eq}) \leqslant \beta\overline{w}. \tag{6}$$

We stress that Eq. (6) is a direct consequence of Eq. (4), and hence it holds regardless of the regime of motion of the system, overdamped or underdamped in all generality. Even the physical nature of the periodic degree is freedom is generic, meaning that $\phi$ may be a geometrical variable, an abstract internal coordinate of the system, or even a dynamical variable (in the underdamped case).

At the computational level, some suitable functional form has to be assigned to $\rho(\phi)$ in order to get a workable expression of Eq. (6). A helpful route might be to express $\rho(\phi)$ as

$$\rho(\phi) = \rho_{\rm eq}(\phi) e^{\Psi(\phi) - \ln\langle e^{\Psi}\rangle_{\rm eq}}, \tag{7}$$

where the compact notation $\langle f\rangle_{\rm eq} \equiv \int_0^{2\pi} d\phi f(\phi)\rho_{\rm eq}(\phi)$ is adopted to indicate equilibrium averages of functions of $\phi$, and where $\Psi(\phi)$ is an associated function which makes Eq. (7) an identity. In practice, $\Psi(\phi) \equiv K + \ln[\rho(\phi)/\rho_{\rm eq}(\phi)]$, where the constant $K$ corresponds to $\ln\langle e^{\Psi}\rangle_{\rm eq}$. The normalization $\int_0^{2\pi} d\phi\, \rho(\phi) = 1$ is assured by construction. By using Eq. (7) to express the relative entropy, a few algebraic steps lead to get $\mathcal{D}(\rho||\rho_{\rm eq}) = \langle \Psi e^{\Psi}\rangle_{\rm eq}/\langle e^{\Psi}\rangle_{\rm eq} - \ln\langle e^{\Psi}\rangle_{\rm eq}$. Thus, Eq. (6) becomes

$$\frac{\langle \Psi e^{\Psi}\rangle_{\rm eq}}{\langle e^{\Psi}\rangle_{\rm eq}} - \ln\langle e^{\Psi}\rangle_{\rm eq} \leqslant \beta\overline{w}. \tag{8}$$

In all generality, the periodicity on the variable $\phi$ allows one to expand $\Psi(\phi)$ in terms of Fourier components:

$$\Psi_{\mathbf{c}}(\phi) = \sum_{n\geqslant 1} [a_n \cos(n\phi) + b_n \sin(n\phi)], \tag{9}$$

where the array $\mathbf{c}$ collects all parameters $a_1, a_2, \ldots, b_1, b_2, \ldots$ of the expansion (the immaterial flat contribution for $n = 0$ is excluded in the summation). A distribution $\rho(\phi)$ is thus admissible if the set $\mathbf{c}$ is such that Eq. (9) fulfills Eq. (8).

Finally, we stress that $\rho(\phi)$ might be specified by an ensemble of order parameters, that is, the averages $\langle f_1\rangle_\rho, \langle f_2\rangle_\rho, \cdots, \langle f_N\rangle_\rho$ of suitably selected functions $f_1(\phi), f_2(\phi), \ldots, f_N(\phi)$. If such functions are mutually orthogonal (in terms of scalar product in the $\phi$ domain), then the corresponding point in the $N$-dimensional space of the order parameters provides an increasingly sharp identification of $\rho(\phi)$ as the set of functions is ever more enlarged. Conversely, low-dimensional representations in the space of a few order parameters give a fuzzy statistical specification which, however, might catch some peculiar features of $\rho(\phi)$.

### B. Unbiased periodic coordinates

So far our discussion has been general. Henceforth we focus on the case of an *a priori* unbiased periodic coordinate, i.e., $\rho_{\rm eq}(\phi) = 1/2\pi$. Concerning the order parameters adopted as descriptors of $\rho(\phi)$, we focus here only on the first-rank order parameters $\langle\cos\phi\rangle_\rho$ and $\langle\sin\phi\rangle_\rho$. If the system were transformed infinitely slowly, then at completion of the cycle all values $\phi$ would be again equiprobable [since $\rho(\phi) \equiv \rho_{\rm eq}(\phi) = 1/2\pi$] so that $\langle\cos\phi\rangle_\rho = \langle\sin\phi\rangle_\rho = 0$; on the contrary, for finite-time transformations, these averages are generally non-null. The global polarization parameter

$$\mathcal{P}_\rho = \sqrt{\langle\cos\phi\rangle_\rho^2 + \langle\sin\phi\rangle_\rho^2} \tag{10}$$

is adopted here to quantify the statistical polarization of the nonequilibrium distribution on $\phi$ [11]. The subscript $\rho$ serves to remark the functional dependence on the distribution $\rho(\phi)$. By construction, $0 \leqslant \mathcal{P}_\rho \leqslant 1$. For infinitely slow transformations, $\mathcal{P}_\rho = 0$ and the system is not statistically polarized. On the opposite side, a value of $\mathcal{P}_\rho$ tending to 1 indicates that the transformation occurred in a finite time and that the system is largely polarized in the sense that the final distribution is peaked around a *certain* value of $\phi$. Note that $\mathcal{P}_\rho$ does not give information about the direction of the polarization.

Now consider the situation in which both the nature of the external agent and the kind of transformation are totally unspecified. Accordingly, the candidate distribution $\rho(\phi)$ may span the whole functional space under the constraint that Eq. (6) [or, equivalently, Eq. (8)] holds for the given $\overline{w}$. The following parameter in then taken as a measure of the *maximum allowed statistical polarization*:

$$\mathcal{P}_{\rm max} = \max_{\text{allowed }\rho} \{\mathcal{P}_\rho\}, \tag{11}$$

where "allowed $\rho$" means that the condition Eq. (6) must be fulfilled. A practical formulation is achieved, for instance, by adopting the parametrization of $\rho(\phi)$ based on Eq. (7) with Eq. (9); by denoting with $\mathcal{P}_{\mathbf{c}}$ the polarization parameter computed with the distribution $\rho(\phi)$ parametrized by the set $\mathbf{c}$, Eq. (11) becomes $\mathcal{P}_{\rm max} = \max_{\text{allowed }\mathbf{c}} \{\mathcal{P}_{\mathbf{c}}\}$, where "allowed $\mathbf{c}$" means that the condition Eq. (8) must be fulfilled.

In practice, $\mathcal{P}_{\rm max}$ sets the maximum value of the polarization parameter in response to a cyclic transformation, given only that the average work per cycle is fixed to $\overline{w}$. Note that $\mathcal{P}_{\rm max}$ is a universal and well-defined function of $\overline{w}$.

For the present case of unbiased periodic coordinate, the exact profile of $\mathcal{P}_{\rm max}$ versus $\beta\overline{w}$ can be found by noticing that a von Mises distribution [5] suitably parametrized is the

resolvent of Eq. (11) under the imposed constraint. The von Mises distribution, $\rho_{\mathrm{vM}}(\phi)$, has the form

$$\rho_{\mathrm{vM}}(\phi) = \frac{1}{2\pi\, I_0(\kappa)}\, e^{\kappa\, \cos(\phi-\mu)}, \tag{12}$$

where $\mu$ is the mean orientation and $\kappa \geqslant 0$ quantifies the orientational concentration about the mean; finally, here and below, $I_n(\cdot)$ is the $n$th-order modified Bessel function of the first kind [12]. The von Mises distribution is unimodal, centered at the value $\mu$, and symmetric. For $\kappa \to 0$ it tends to the uniform distribution, while in the opposite limit of large $\kappa$ it is well approximated by a Gaussian profile of variance $\kappa^{-1}$. The key point is to recognize that $\rho_{\mathrm{vM}}(\phi)$ is the distribution with the maximum information entropy at given mean resultant length (which corresponds to the polarization parameter in our context) [13]. This implies that $\rho_{\mathrm{vM}}(\phi)$ *minimizes* the relative entropy with respect to $\rho_{\mathrm{eq}}(\phi) = 1/2\pi$ at fixed $\mathcal{P}$. For the von Mises distribution, the relative entropy and the polarization parameter have explicit expressions, namely $\mathcal{D}(\rho_{\mathrm{vM}}||\rho_{\mathrm{eq}}) = \kappa\, I_1(\kappa)/I_0(\kappa) - \ln I_0(\kappa)$ and $\mathcal{P} = I_1(\kappa)/I_0(\kappa)$. Now consider that fixing $\mathcal{P}$ corresponds to fix $\kappa$, and that both $\mathcal{D}(\rho_{\mathrm{vM}}||\rho_{\mathrm{eq}})$ and the polarization parameter monotonically increase with $\kappa$. Thus, to determine $\mathcal{P}_{\mathrm{max}}$ from Eq. (6), it suffices to solve the equation

$$\kappa\, \frac{I_1(\kappa)}{I_0(\kappa)} - \ln I_0(\kappa) = \beta \overline{w} \tag{13}$$

with respect to $\kappa \geqslant 0$, and then compute

$$\mathcal{P}_{\mathrm{max}} = \frac{I_1(\kappa)}{I_0(\kappa)}. \tag{14}$$

Note that the parameter $\mu$ does not enter the above expressions. This agrees with the fact that only the extent of the polarization can be determined but not its direction.

The profile of $\mathcal{P}_{\mathrm{max}}$ versus $\beta\overline{w}$ resulting from the numerical solution of Eqs. (13) and (14) is displayed in Fig. 1 in a double-logarithmic scale. What emerges is that $\mathcal{P}_{\mathrm{max}} \simeq \sqrt{\beta\overline{w}}$ for $\beta\overline{w} \leqslant 1$, while for $\beta\overline{w}$ exceeding 1 the profile bends tending to the limit value 1. Roughly, the behavior on the whole energy scale is found to follow closely

$$\mathcal{P}_{\mathrm{max}} \simeq \sqrt{\tanh\left(\beta\overline{w}\right)}, \tag{15}$$

which corresponds to the dashed line in Fig. 1. The adoption of $\tanh(\cdot)$ relies only on the fact that such a simple function well captures the features of the exact solution. The inset shows the percentage relative deviation of $\sqrt{\tanh\left(\beta\overline{w}\right)}$ from the true values. Note that Eq. (15) is globally accurate within 3% and that, more importantly, it gives an *overestimation* of $\mathcal{P}_{\mathrm{max}}$ in the whole range of $\beta\overline{w}$ values [14]. On this basis we can safely make the following assertion:

(ii) *Given that an external agent expends on average an amount of energy* $\overline{w}$ *per cycle, the system's polarization parameter* $\mathcal{P}$ *over an a priori unbiased periodic degree of freedom cannot be larger than* $\sqrt{\tanh\left(\beta\overline{w}\right)}$.

We underline the important fact that such a statement holds, exactly as the starting point represented by Eq. (4), regardless of the system's regime of motion (overdamped or underdamped) and of the physical nature of the variable $\phi$. In fact, all steps from Eq. (4) to Eq. (6) to statement (ii) are sequential and the level of validity is preserved. On this

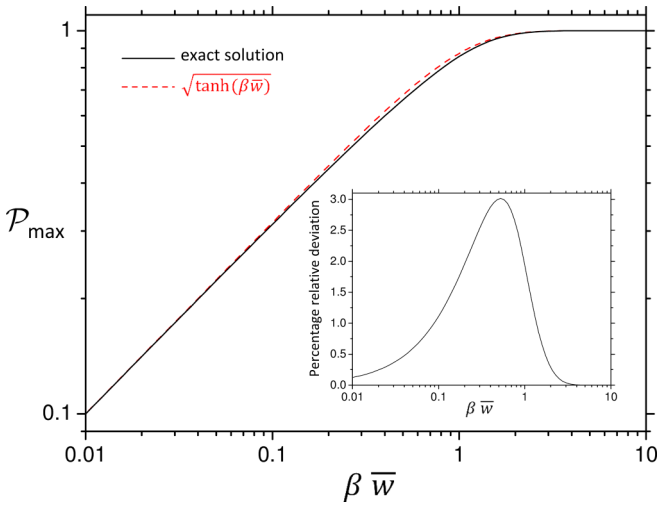


FIG. 1. Maximum polarization parameter $\mathcal{P}_{\mathrm{max}}$ versus the average performed work per cycle (equal to the average dissipated energy) for the case of single unbiased periodic coordinate. The exact solution is displayed with continuous line, while the dashed line corresponds to $\sqrt{\tanh(\beta\overline{w})}$ that closely approximates the exact profile from above. The inset shows the percentage relative deviation of $\sqrt{\tanh(\beta\overline{w})}$ from the true values. (Because of overflow issues in the computation of the Bessel's functions of large arguments, for $\beta\overline{w}$ greater than 3.7 the values of $\mathcal{P}_{\mathrm{max}}$ have been computed by employing the approximation given in the note Ref. [14].)

basis, the strength of statement (ii) lies in the possibility to apply it *directly* to any situation in which the requirements for Eq. (4) (Markov character of the dynamics and validity of the microreversibility even in out-of-equilibrium conditions) are fulfilled at least as good approximations and, of course, under condition that an internal periodic coordinate $\phi$ is present. System's specific details are not required. In Sec. V we shall provide an example of direct application of statement (ii) to a situation of potentially wide interest.

It is worth to highlight that the statement (ii) can be reformulated as follows: *To have a chance to achieve a certain degree of polarization* $\mathcal{P}$*, one has to perform an average amount of work* $\overline{w} \geqslant \beta^{-1} \tanh^{-1}(\mathcal{P}^2)$. Since the work is a measurable quantity, this assertion may be useful to identify the experimental conditions that *may* allow the realization of a nonequilibrium distribution with the target polarization at the end of the cycle. The relation given above shows that the higher the target polarization, the higher must be $\overline{w}$ for having the chance to achieve it. By recalling that for cyclic transformations $\overline{w}$ corresponds to the average energy dissipation, this also means that the higher degree of polarization is associated with higher dissipation. Such a viewpoint might have a practical relevance in the context of single-system manipulations by considering that $\mathcal{P}$ quantifies the precision on the localization of $\phi$ with respect to the mean (expectation) value; our finding gives the *a priori* minimum average energy cost, or dissipation, for having the chance to reach a desired precision in response to the cyclic transformation.

Although the exact solution is obtainable as described above, we believe that it is worthwhile to present also a numerical methodology aiming to get an estimate of $\mathcal{P}_{\mathrm{max}}$ by means of a random search in the space of the parameters

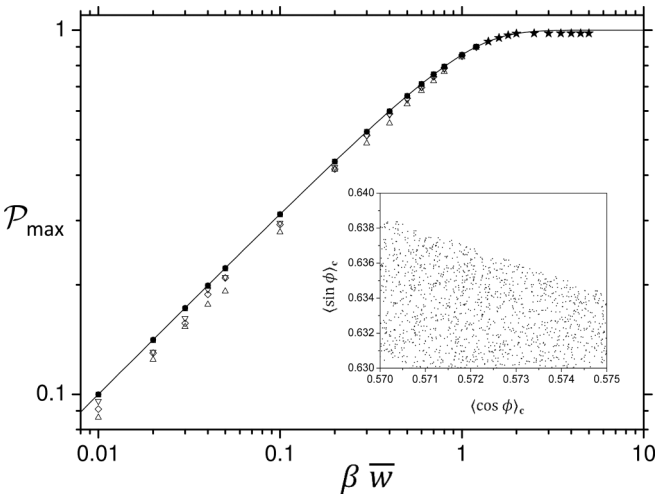


FIG. 2. Maximum polarization parameter versus the average performed work per cycle for the case of single unbiased periodic coordinate: outcomes from the numerical inspection. The different symbols correspond to different setup parameters employed in the calculations (see the Appendix for details). In all cases, $R_{max} = 10$ and $N_{sectors} = 500$ (calculations with $N_{sectors} = 50$ give comparable results). Then, the different choices are $n_{max} = 1$, $N_{trials}(1) = 10^6$ (filled circles); $n_{max} = 1$, $N_{trials}(1) = 10^5$ (open circles); $n_{max} = 2$, $N_{trials}(1) = 10^6$ (squares); $n_{max} = 4$, $N_{trials}(1) = 10^6$ (rhombuses); $n_{max} = 5$, $N_{trials}(1) = 10^6$ (triangles); $n_{max} = 5$, $N_{trials}(1) = 10^8$ (down-triangles). The stars beyond $\beta\overline{w} = 1.2$ refer to $n_{max} = 4$, $N_{trials}(1) = 10^5$; the outcomes for $\beta\overline{w} \geqslant 2.5$ are limited by the cutoff on $\mathcal{P}_{max}$ set to 0.98. The continuous line corresponds to the exact solution also shown in Fig. 1. The inset shows the density of points in a small portion of the plane of the averages $\langle \sin\phi \rangle_{\mathbf{c}}$ and $\langle \cos\phi \rangle_{\mathbf{c}}$; each point corresponds to a set $\mathbf{c}$ for which Eq. (8) is fulfilled. Such a pattern refers to the setup corresponding to the filled circles and $\beta\overline{w} = 1.0$. The full bi-dimensional diagram, here not shown, appears to be a compact circular region (in accord with the physical invariance with respect to arbitrary angular shifts) densely filled and centered in (0,0).

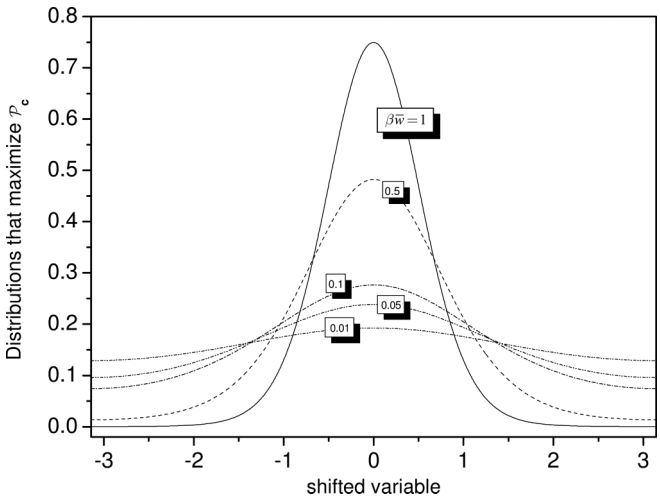


FIG. 3. Distributions $\rho_{\mathbf{c}}(\phi)$ that maximize $\mathcal{P}_{\mathbf{c}}$ for various values of $\beta\overline{w}$. For each distribution, the abscissa is shifted with respect to the point of maximum. The outcomes refer to the search with $n_{max} = 1$, $N_{sectors} = 500$, $N_{trials}(1) = 10^5$ (open circles in Fig. 2).

**c** which specify $\rho(\phi)$ through Eq. (7) with Eq. (9); the computational details are given in the Appendix. In essence, for each set **c** it is checked if the candidate distribution fulfills the requisite of Eq. (8). If the check is passed, then any property of the distribution (for example, the polarization parameter of interest here) can be computed for that allowed set **c**. The random search in the **c** space might be useful to treat the cases in which $\rho_{eq}(\phi)$ is nonuniform and the exact solution is not attainable.

In the present application, the numerical determination of the maximum polarization at given $\beta\overline{w}$ is performed by individuating, among all sets **c** that fulfill Eq. (8), the set that yields the maximum value of $\mathcal{P}_{\mathbf{c}}$. Clearly, any search in the parameter space can provide only an estimate *from below* of the maximum polarization. However, as the search is ever more exhaustive, such an estimate is expected to converge asymptotically to the value $\mathcal{P}_{max}$, which can be hence obtained by a plausible extrapolation. The results are shown in Fig. 2. The spread of the outcomes is ascribable to the different computational setups, in particular to the maximum rank of the Fourier components when a truncated version of Eq. (9) is adopted in practice. The closeness of the outcomes to the exact solution (the continuous line) demonstrates that the strategy is effective. It is found that limiting the summation to first-rank components suffices to span efficiently the family of candidate distributions $\rho(\phi)$. The inclusion of higher-rank components does not bring relevant improvements and requires an ever more intensive sampling which rapidly becomes prohibitive. In the light of the analytic treatment described above, such a trend is readily explained by considering that a single first-rank Fourier component enters the von Mises distribution. Thus, including components of higher rank only leads to a worsening of the outcomes since the random search is spread over irrelevant dimensions.

Figure 3 shows, for some values $\beta\overline{w}$, the distribution $\rho(\phi)$ corresponding to the set of parameters **c** that yields the highest value of $\mathcal{P}_{\mathbf{c}}$; a single Fourier component has been considered in the search. The profiles are displayed versus the variable $\phi$ shifted with respect to the point of maximum. Note that all the features of von Mises distribution are present and, as expected, the profiles become narrower and well approximated by a Gaussian as $\beta\overline{w}$ is ever larger (that is, at increasing maximum polarization). As a check, we have verified that the profiles of $\rho_{vM}(\phi)$ computed with $\kappa$ corresponding to $\beta\overline{w}$ (for example, $\kappa = 1.789$ for $\beta\overline{w} = 0.5$) are indistinguishable from those of Fig. 3 under the graphical resolution.

### C. Numerical example

Just for illustrative purposes, let us consider a numerical realization of a cyclic transformation on an unbiased unidimensional rotor with angular degree of freedom $\phi$. For $0 \leqslant t \leqslant \tau$ with $\tau$ the duration of the cycle, let $V_t(\phi)$ be the time-dependent system's energy due to the interaction with some external means. In this example, the same kind of energy modulation already considered in previous studies [9,15] is applied: $\beta V_t(\phi) = \Delta\,\epsilon(t)\,\cos[\phi + 0.7\epsilon(t)]$ with $\epsilon(t) = \sin(2\pi t/\tau)$ and $\Delta = 4$. By assuming overdamped motion with constant diffusion coefficient $D$, the

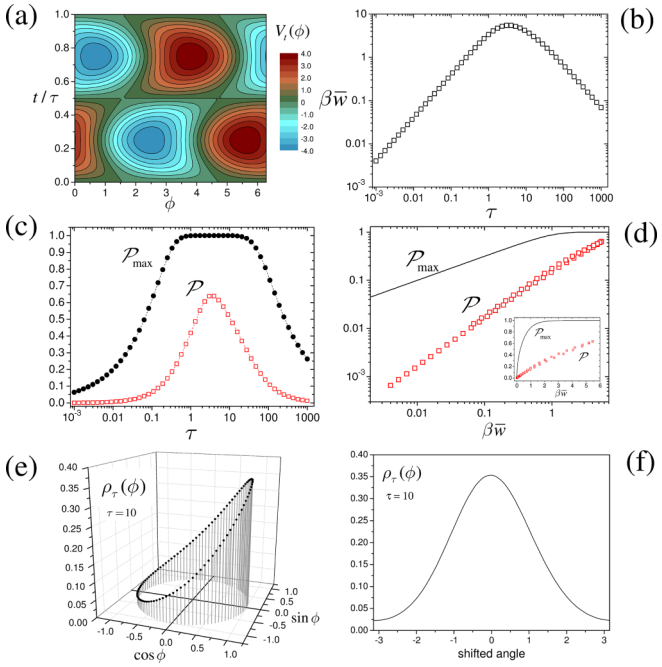


FIG. 4. Example of statistical polarization for the unbiased unidimensional overdamped rotor described in Sec. IV C. Panel (a) shows the energy modulation during the transformation cycle. Panel (b) shows $\beta\overline{w}$ versus the cycle duration $\tau$ in double-logarithmic scale. Panel (c) displays the polarization parameter versus $\tau$; red squares refer to $\mathcal{P}$ and black circles to $\mathcal{P}_{\max}=\sqrt{\tanh(\beta\overline{w})}$ computed for $\beta\overline{w}$ corresponding to the given $\tau$. Panel (d) displays $\mathcal{P}$ and $\mathcal{P}_{\max}$ in the same fashion of Figs. 1 and 2; the same profiles in linear scale are shown in the inset. Panel (e) shows the nonequilibrium distribution $\rho_\tau(\phi)$ at the end of the cycle of duration $\tau=10$. Panel (f) displays the same distribution in the fashion of Fig. 3, that is, with the angular variable shifted with respect to the point of maximum of the distribution (the maximum falls at 0.346 rad).

nonequilibrium distribution $\rho_t(\phi)$ evolves according to the nonstationary Fokker-Planck equation $\partial\rho_t(\phi)/\partial t=-\hat{\Gamma}(t)\rho_t(\phi)$, where $\hat{\Gamma}(t)=-D\frac{\partial}{\partial\phi}e^{-\beta V_t(\phi)}\frac{\partial}{\partial\phi}e^{\beta V_t(\phi)}$ is the time-dependent Smoluchowski operator [16]; the initial condition is $\rho_0(\phi)=1/2\pi$. Such an equation has been solved numerically by means of a finite-difference scheme with homogeneous partition of the domain of the angle $\phi$, and employing the forward Euler propagation route [17] (for details, see Ref. [15]). The average work at completion of the cycle is then achieved by computing numerically the double integral $\beta\overline{w}=\int_0^\tau dt\int_0^{2\pi}d\phi\,\rho_t(\phi)\partial[\beta V_t(\phi)]/\partial t$. For each value $\tau$, the polarization parameter at the end of the cycle, $\mathcal{P}=\sqrt{\langle\cos\phi\rangle_\tau^2+\langle\sin\phi\rangle_\tau^2}$, is also obtained by computing numerically the required integrals $\langle\cos\phi\rangle_\tau=\int_0^{2\pi}d\phi\,\rho_\tau(\phi)\cos(\phi)$ and $\langle\sin\phi\rangle_\tau=\int_0^{2\pi}d\phi\,\rho_\tau(\phi)\sin(\phi)$.

Figure 4 collects the results. Figure 4(a) shows the energy modulation during the cycle. The profile of $V_t(\phi)$ features a single asymmetric well whose shape, depth, and point of minimum all change during the cycle; at $t=0$, $t=\tau/2$, and $t=\tau$, the energy profile is flat. Figure 4(b) reports $\beta\overline{w}$ versus $\tau$. The double-logarithmic scale helps to recognize the increase $\beta\overline{w}\propto\tau$ for short cycles and the decrease $\beta\overline{w}\propto\tau^{-1}$ for long cycles, while a maximum falls at a certain duration of the cycle. Such general features of the profiles of $\beta\overline{w}$ versus $\tau$ have been discussed in Ref. [15]. Figure 4(c) shows the profile of the polarization parameter versus the duration of the cycle. The red squares refer to $\mathcal{P}$, while the black circles are the values of $\mathcal{P}_{\max}=\sqrt{\tanh(\beta\overline{w})}$ computed for $\beta\overline{w}$ corresponding to the given $\tau$. Note that, as expected, the entire profile of $\mathcal{P}$ lies below the profile of $\mathcal{P}_{\max}$. Figure 4(d) displays the same information in the fashion of Figs. 1 and 2. As a whole, the actual polarization parameter $\mathcal{P}$ never falls above $\mathcal{P}_{\max}$. Finally, Fig. 4(e) shows the nonequilibrium distribution at the end of the cycle, $\rho_\tau(\phi)$, for $\tau=10$, which is close to the condition of maximum average dissipation [see Fig. 4(b)]. The system's statistical polarization induced by the transformation clearly emerges from the shape of such a distribution which results to be peaked at the angle 0.346 rad. Figure 4(f) shows the distribution in the same way of the profiles in Fig. 3, that is, by shifting the angular variable with respect to the point of maximum. Although this profile might resemble those of Fig. 3, $\rho_\tau(\phi)$ is very far from the von Mises distribution that realizes the maximum polarization. In fact, for $\tau=10$ we have $\beta\overline{w}\simeq 3.4$ corresponding to $\mathcal{P}_{\max}\simeq 1$ in Fig. 4(d); the von Mises distribution that yields such a high maximum polarization would appear as an extremely sharp peak [$\kappa=1278$ in Eq. (12)].

## V. POLARIZATION OF THE VELOCITIES IN A MANY-BODY SYSTEM

Let us consider a generic cyclic transformation performed on a system constituted by pointlike massive moieties; for example, it might be a molecular system in fully atomistic or united-atom representations. The generic variables $\mathbf{x}$ here correspond, in a phase-space representation, to the set of positional coordinates (with reference to a chosen frame of axes) along with the associated velocities. The dynamics of $\mathbf{x}$ are assumed to be a multidimensional Markov process, possibly described by a Langevin equation in the underdamped regime.

Let us focus on one of the moieties. Given an arbitrarily chosen observation plane, the angular distribution of the projection of the velocity of that moiety onto the observation plane is clearly uniform at the thermal equilibrium [18]. On the contrary, a statistical polarization is expected at the completion of the cycle. A pictorial representation of this situation is given in Fig. 5. The in-plane orientation of the velocity can be specified by an angular variable which behaves exactly as the periodic coordinate $\phi$ considered above. Thus, all previous findings are inherited in the present case and, in particular, the statement (ii) is readily adapted as follows:

(iii) *Consider a many-body system made of pointlike massive moieties and choose an observation plane; if an external agent acts on the system and performs a cyclic transformation by expending an average amount of energy $\overline{w}$, the polarization parameter $\mathcal{P}$ for the projection of the velocity of a moiety onto the observation plane cannot be larger than $\sqrt{\tanh(\beta\overline{w})}$.*

Such a statement is valid in all generality: it holds regardless of the complexity of the system and of the features of the internal configurational energetics, regardless of the number of the moieties and also regardless of their masses.

Finally, note that $\mathcal{P}$ is also a measure of the in-plane coherent movement that can be realized in an ensemble of

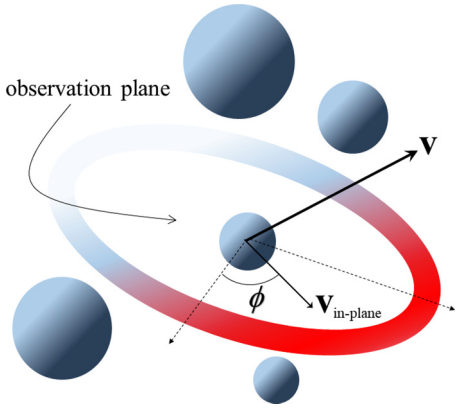


FIG. 5. Pictorial representation of the in-plane angular polarization of the velocity vector for a moiety of a fluctuating system after a cyclic transformation. The azimuthal angle $\phi$ is the (*a priori* unbiased) periodic degree of freedom of interest. The shaded color represents, in abstract way, the polarization which is induced by a cyclic transformation performed on the system.

system's replicas all subjected in parallel to the same cyclic transformation. In fact, by focusing on a certain moiety, the direction of the velocity polarization (although not known) is the same for all replicas. Thus, $\mathcal{P}$ gives the extent of coherence of the induced motion onto the observation plane. This point of view may be of interest if the external agent is some field that interacts simultaneously with many replicas of the same system.

## VI. CONCLUDING REMARKS

In this work we have pointed out that Eq. (3) can be viewed as a constraint to establish, for a fluctuating system transformed in contact with a thermal bath and initially at equilibrium, which final nonequilibrium distributions $p(\mathbf{x})$ are admissible, and which are not, just on the basis of the amount of energy dissipated on average. Characterizing the deviation of $p(\mathbf{x})$ from $p_{\text{eq}}(\mathbf{x})$ could be crucial for the understanding of the operation at the nanoscale, for example, in "one-shot" molecular machines [19], which can be ascribed to complex supra-molecular structures responding to external stimuli and using input energy to execute a certain function. The line pursued here consists in mapping the low-dimensional space of a few order parameters which are supposed to catch relevant features of $p(\mathbf{x})$, and then finding the portion of such a space which is allowed at the given average dissipation.

The practical implementation of this concept becomes relatively simple when dealing with cyclic transformations, so that the average dissipation is directly identified with the average performed work [hence Eq. (3) is replaced by Eq. (4)], and when the focus is on reduced distributions on single degrees of freedom [use of Eq. (5)]. This is exactly the case elaborated here. Among all possible situations, we opted to inspect systems possessing a periodic degree of freedom over which the equilibrium distribution is uniform. An upper bound to the amount of statistical polarization on such a kind of coordinate was obtained as a function of the average work (hence of average energy dissipated) per cycle. The exact solution has been achieved by recognizing that the von Mises distribution is exactly the resolvent of the key relation Eq. (6) for this specific problem. Notably, with the exact solution at hand we could validate the effectiveness of a proposed numerical strategy that might prove useful to face the general case of periodic coordinates with nonuniform equilibrium distribution, for which the exact solution is not attainable. The example in Sec. IV C illustrates that the general expectations are met for the case of unidimensional overdamped rotor subjected to a cyclic energy modulation (here arbitrarily chosen).

As first application of Eq. (15), we have estimated the maximum extent of the velocity polarization that can be induced on a massive moiety of a system subjected to a generic cyclic transformation. The ubiquity of such a situation, which concerns all many-body classical fluctuating systems, justifies our first choice of focusing on the case of periodic degrees of freedom that are unbiased at the equilibrium.

The present analysis can be easily repeated for degrees of freedom with nonuniform equilibrium distribution and/or by considering other sets of order parameters in place of the first-rank ones employed here to explore the polarization feature. Furthermore, we emphasize that the same methodological approach can be pursued, at least in principle, to treat different situations at increasing levels of complexity, possibly considering a larger number of degrees of freedom.

## APPENDIX: RANDOM SEARCH IN THE PARAMETER SPACE

It is here illustrated the strategy to perform a random search in the space of the parameters $\mathbf{c}$ specifying the distribution $\rho(\phi)$ through Eq. (7) with Eq. (9) under the constraint in Eq. (8). The specific target is to get an estimate of $\mathcal{P}_{\max}$ for a given value of $\beta\overline{w}$.

In the computational setup, the maximum allowed rank of the Fourier components is set to a value $n_{\max}$, hence $1 \leqslant n \leqslant n_{\max}$ in Eq. (9). The sampling of the $2 \times n_{\max}$ expansion coefficients $a_1, a_2, \ldots, a_{\max}, b_1, b_2, \ldots, b_{\max}$, collected in the array $\mathbf{c}$, was performed as described in the following. We stress that since the purpose is only to explore the $\mathbf{c}$ space for detecting the maximum of $\mathcal{P}_{\mathbf{c}}$, any sampling strategy is allowed, at condition that the $\mathbf{c}$ space be well explored (this has to be checked by varying the parameters of the computational setup).

Let us introduce $R = \sqrt{\sum_n a_n^2 + b_n^2}$ and choose a cutoff value $R_{\max}$. Note that $R$ can be interpreted as the distance, from the origin, of a point $\mathbf{c}$ in a $(2 \times n_{\max})$-dimensional ball of radius $R_{\max}$. Let $N_{\text{sectors}}$ be the number of sectors, of equal width $\Delta = R_{\max}/N_{\text{sectors}}$, into which the segment $[0, R_{\max}]$ is divided. The $i$th sector $(1 \leqslant i \leqslant N_{\text{sectors}})$ corresponds to values $(i-1)\Delta < R \leqslant i\Delta$. The number of trials assigned to each sector was set to increase linearly according to $N_{\text{trials},i} = N_{\text{trials}}(1)\,\Delta^2\,(2i-1)$, where $N_{\text{trials}}(1)$ corresponds to a given number of trials within the ball of radius $R = 1$. The adoption of such a linear growth is a subjective choice. Such a weak increase of $N_{\text{trials},i}$ implies that the sampling of the $\mathbf{c}$ space is not uniform (it would be uniform only if the number of components of $\mathbf{c}$ were equal to 3) and ever more rarefied as $R$ increases. This choice was done in purpose to privilege the sampling in the region likely associated with smooth distributions $\rho_{\mathbf{c}}(\phi)$ having a bigger chance to pass the check

of Eq. (8). In fact, as $R$ is ever larger, the probability of generating very irregular distributions is expected to increase [since a large weight may be assigned to Fourier components with large $n$ in Eq. (9)], leading to a high rejection ratio.

For each value of $\overline{w}$, the following procedure was adopted. Per each sector, a trial is made by generating a set $\mathbf{c}$ with components $a_n = \alpha_n[(i-1)\Delta + \gamma\Delta]/\mathcal{N}$ and $b_n = \beta_n[(i-1)\Delta + \gamma\Delta]/\mathcal{N}$, where the number $\gamma$ is randomly drawn from the uniform distribution in [0,1], $\alpha_n$ and $\beta_n$ are randomly drawn from the uniform distribution in $[-1/2, 1/2]$, and $\mathcal{N} = \sqrt{\sum_n \alpha_n^2 + \beta_n^2}$. In such a way, the value of $R$ falls in the $i$th sector. Given $\mathbf{c}$, the condition Eq. (8) is checked. If such a condition is fulfilled, then the averages $\langle\cos\phi\rangle_{\mathbf{c}}$ and $\langle\sin\phi\rangle_{\mathbf{c}}$, and the polarization parameter $\mathcal{P}_{\mathbf{c}} = \sqrt{\langle\sin\phi\rangle_{\mathbf{c}}^2 + \langle\cos\phi\rangle_{\mathbf{c}}^2}$, are computed. The maximum value of $\mathcal{P}_{\mathbf{c}}$ is updated after each accepted trial. The search is interrupted if the number of accepted trials in the actual sector falls below 5% or if $\mathcal{P}_{\mathbf{c}}$ exceeds a threshold value (here set to 0.98) which is applied to stop lengthy calculations; otherwise, the search continues up to explore all the sectors. For all calculations of Fig. 2, the cutoff $R_{\max}$ was set to the value 10. With such a choice it happened that the search, in all cases, was automatically interrupted at a certain sector whose number was found to be ever larger as $\beta\overline{w}$ increases. This indicates that $R_{\max} = 10$ is sufficiently high to assure an exhaustive search in the $\mathbf{c}$ space. Random numbers were generated by means of the Fortran subroutine "ran2" [20]. To avoid correlations, the computations have been carried out independently for each value of $\overline{w}$. The numerical integrations were performed by means of a subroutine employing Romberg's method. A Fortran code has been developed to perform the calculations.

In summary, the setup parameters are $n_{\max}$, $R_{\max}$, $N_{\text{sectors}}$, and $N_{\text{trials}}(1)$. Although the sampling strategy described above is subjective, the important fact to check is that the outcomes have a converging trend with respect to independent variations of the setup parameters. This indeed occurs in the present application.


[1] C. Jarzynski, Equalities and inequalities: Irreversibility and the second law of thermodynamics at the nanoscale, Annu. Rev. Condens. Matter Phys. **2**, 329 (2011).

[2] J. L. England, Dissipative adaptation in driven self-assembly, Nat. Nanotechnol. **10**, 919 (2015).

[3] N. Perunov, R. A. Marsland, and J. L. England, Statistical Physics of Adaptation, Phys. Rev. X **6**, 021036 (2016).

[4] M. Nguyen and S. Vaikuntanathan, Design principles for nonequilibrium self-assembly, Proc. Natl. Acad. Sci. USA **113**, 14231 (2016).

[5] K. V. Mardia, *Directional Statistics* (John Wiley & Sons, New York, 2000).

[6] S. Kullback and R. A. Leibler, On information and sufficiency, Ann. Math. Stat. **22**, 79 (1951).

[7] For completeness, we mention that since the average dissipated energy equals the average heat released to the thermal bath during the transformation, the quantity $\overline{w}/T$ gives the contribution to the average increase of the environment's entropy in the active part of the cycle (a further contribution comes from the heat exchanged between system and environment in the subsequent free relaxation phase to equilibrium).

[8] S. Vaikuntanathan and C. Jarzynski, Dissipation and lag in irreversible processes, Europhys. Lett. **87**, 60005 (2009).

[9] D. Frezzato, Dissipation, lag, and drift in driven fluctuating systems, Phys. Rev. E **96**, 062113 (2017).

[10] Let us write $p(\mathbf{x}) = \rho(\mathbf{x}_1)p_c(\mathbf{x}_2|\mathbf{x}_1)$ where $p_c(\mathbf{x}_2|\mathbf{x}_1)$ is the conditioned distribution with normalization $\int d\mathbf{x}_2 p_c(\mathbf{x}_2|\mathbf{x}_1) = 1$ for any $\mathbf{x}_1$. Similarly, $p_{\text{eq}}(\mathbf{x}) = \rho_{\text{eq}}(\mathbf{x}_1)p_{c,eq}(\mathbf{x}_2|\mathbf{x}_1)$. By inserting these forms into Eq. (1) gives

$$\mathcal{D}(p||p_{\text{eq}}) = \mathcal{D}(\rho||\rho_{\text{eq}}) + \int d\mathbf{x}_1 \rho(\mathbf{x}_1)\left[\int d\mathbf{x}_2 p_c(\mathbf{x}_2|\mathbf{x}_1)\ln\frac{p_c(\mathbf{x}_2|\mathbf{x}_1)}{p_{c,\text{eq}}(\mathbf{x}_2|\mathbf{x}_1)}\right].$$

Since the quantity within curly brackets is non-negative for any $\mathbf{x}_1$ (it is the relative entropy for the conditioned distributions), also the integral is non-negative and Eq. (5) follows.

[11] To justify such a statement, consider a direction of inspection identified by the angle $\alpha$. The average $\langle\cos(\phi-\alpha)\rangle_\rho$ represents the polar orientational order parameter with respect to that direction. By using the definition Eq. (10), it follows $\langle\cos(\phi-\alpha)\rangle_\rho = \mathcal{P}_\rho \times (c\cos\alpha - s\sin\alpha)$ where $c = \langle\cos\phi\rangle_\rho/\sqrt{\langle\cos\phi\rangle_\rho^2 + \langle\sin\phi\rangle_\rho^2}$ and $s = \langle\sin\phi\rangle_\rho/\sqrt{\langle\cos\phi\rangle_\rho^2 + \langle\sin\phi\rangle_\rho^2}$. By construction, $|c| \leqslant 1$, $|s| \leqslant 1$ and $c^2 + s^2 = 1$; hence, there exists an angle $\phi^*$ such that both $\phi^* = \arccos c$ and $\phi^* = \arcsin c$ are fulfilled. It follows $\langle\cos(\phi-\alpha)\rangle_\rho = \mathcal{P}_\rho \times (\cos\phi^*\cos\alpha - \sin\phi^*\sin\alpha)$, which implies that the order parameter takes the maximum value, equal to $\mathcal{P}_\rho$, for the direction of inspection corresponding to $\alpha = -\phi^*$. Therefore, for a given distribution $\rho(\phi)$, the value $\max_\alpha\langle\cos(\phi-\alpha)\rangle_\rho \equiv \mathcal{P}_\rho$ quantifies the angular polarization (even though the direction of the polarization is not specified by $\mathcal{P}_\rho$ alone).

[12] M. Abramowitz and I. A. Stegun, *Handbook of Mathematical Functions* (Dover, New York, 1970).

[13] The information entropy of $\rho(\phi)$ is $H_\rho = -\int_0^{2\pi} d\phi\rho(\phi)\ln\rho(\phi)$. The relation between $H_\rho$ and the relative entropy of $\rho(\phi)$ with respect to $\rho_{\text{eq}}(\phi) = 1/2\pi$ is simply $\mathcal{D}(\rho||\rho_{\text{eq}}) = -H_\rho + \ln(2\pi)$. For insights on the fact that $\rho_{\text{vM}}(\phi)$ is the distribution with maximum information entropy at given mean resultant length, we address the reader to pages 42 and 43 of Ref. [5] and references therein.

[14] The limit behaviors of $\mathcal{P}_{\max}$ for $\beta\overline{w} \to 0$ and $\beta\overline{w} \to \infty$ can be found, respectively, by plugging in Eqs. (13) and (14) the approximations of the modified Bessel functions at small and large arguments $\kappa$ (respectively, Eqs. 9.6.10 and 9.7.1 of Ref. [12]). In the low-work limit we get $\mathcal{P}_{\max} \simeq \sqrt{\beta\overline{w}}[1 - \beta\overline{w}/8 + \mathcal{O}((\beta\overline{w})^2)]$, while $\sqrt{\tanh(\beta\overline{w})} \simeq \sqrt{\beta\overline{w}}[1 - (\beta\overline{w})^2/6 + \mathcal{O}((\beta\overline{w})^2)]$. In the high-work limit the result is $\mathcal{P}_{\max} \simeq 1 - \pi e^{-2\beta\overline{w}-1} + \mathcal{O}(e^{-2\beta\overline{w}})$, to be compared with $\sqrt{\tanh(\beta\overline{w})} \simeq 1 - e^{-2\beta\overline{w}} + \mathcal{O}(e^{-2\beta\overline{w}})$. In both limits, the function $\sqrt{\tanh(\beta\overline{w})}$ lies above $\mathcal{P}_{\max}$ with a deviation that tends to vanish as $\beta\overline{w} \to 0$ and $\beta\overline{w} \to \infty$.

[15] F. Camerin and D. Frezzato, Fluctuating systems under cyclic perturbations: Relation between energy dissipation and intrinsic relaxation processes, Phys. Rev. E **94**, 022117 (2016).

[16] C. W. Gardiner, *Handbook of Stochastic Methods*, 3rd ed. (Springer-Verlag, Berlin, 2004).

[17] For the present calculations, the time-step of propagation was fixed to $10^{-5}$ for cycles of duration up to $\tau = 10^{-2}$, and to $10^{-4}$ for larger values of $\tau$. The number of intervals for the partition of the domain of the angle $\phi$ was set to 100. The convergence with respect to the change of these parameters has been checked directly on the values of $\beta\overline{w}$ and $\mathcal{P}$ at the end of the cycles; the above choices assure accuracy within 0.3%.

[18] $p(\mathbf{x})$ is factorized as product of the Boltzmann distribution on the configurational variables, and of Gaussian distributions for each of the Cartesian components of the velocity vectors (Maxwell distribution). With respect to a reference frame whose transverse axes lie on a chosen observation plane, let us express the velocity of the $i$th moiety in spherical coordinates $(v_i, \theta_i, \phi_i)$, where $v_i$ is the velocity modulus, $\theta_i$ is the polar angle and $\phi_i$ is the azimuthal angle. The (Gaussian) Maxwell distribution on the Cartesian components implies the reduced distributions $\rho^v_{\rm eq}(v_i) = (2/\pi)^{1/2}\sigma_i^{-3} {v_i}^2 e^{-{v_i}^2/2\sigma_i^2}$, where $\sigma_i = (\beta m_i)^{-1/2}$ with $m_i$ the mass of the moiety, $\rho^\theta_{\rm eq}(\theta_i) = 2^{-1}\sin\theta_i$, and $\rho^\phi_{\rm eq}(\phi_i) = 1/2\pi$; the normalizations are $\int_0^\infty dv_i\, \rho^v_{\rm eq}(v_i) = 1$, $\int_0^\pi d\theta_i\, \rho^\theta_{\rm eq}(\theta_i) = 1$, and $\int_0^{2\pi} d\phi_i\, \rho^\phi_{\rm eq}(\phi_i) = 1$. The angle $\phi_i$ is the unbiased periodic coordinate of interest.

[19] D. Chowdhury, Stochastic mechano-chemical kinetics of molecular motors: A multidisciplinary enterprise from a physicist's perspective, Phys. Rep. **529**, 1 (2013).

[20] W. H. Press, S. A. Teukolsky, W. T. Vetterling, and B. P. Flannery, *Numerical Recipes in Fortran 77: The Art of Scientific Computing*, Vol. 1, 2nd ed. (Cambridge University Press, New York, 1992).